water

MDPI

Article

Study on Parameters of Two Widely Used Cohesive Soils Erosion Models

Qiusheng Wang *,†, Pengzhan Zhou, Junjie Fan and Songnan Qiu

The Key Laboratory of Urban Security and Disaster Engineering of Ministry of Education, Beijing University of Technology, Beijing 100124, China; zhou.p.z@foxmail.com (P.Z.); fan.jmore@foxmail.com (J.F.); qiusn@emails.bjut.edu.cn (S.Q.)

* Correspondence: wangqs@bjut.edu.cn

† Current address: College of Architecture and Civil Engineering, Beijing University of Technology, No.100, Pingleyuan, Chaoyang District, Beijing 100124, China.

Abstract: The erosion rate of cohesive soils was typically modeled with the excess shear stress model and the Wilson model. Several kinds of research have been conducted to determine the erodibility parameters of the two models, but few attempts have been made hitherto to investigate the general trends and range of the erodibility parameter values obtained by the commonly used Erosion Function apparatus. This paper collected a database of 177 erosion function apparatus tests to indicate the variability of all erodibility parameters; the range of erodibility parameters is determined by data statistics and parameter theoretical value derivation. The critical shear stress (τ_c) and erodibility coefficient (Z_0) in the over-shear stress model have a positive proportional relationship when the data samples are sufficient. However, there is no such relationship between the erodibility coefficient (b_0) and erodibility coefficient (b_1) in the Wilson model. It is necessary to express the soil erosion resistance by considering all erosion parameters in the erosion model. Equations relating erodibility parameters to water content, plasticity index, and median particle size were developed by regression analysis.

Keywords: cohesive soils; detachment rate model; soil erosion; erodibility parameter; regression analysis; erosion function apparatus

check for updates

Citation: Wang, Q.; Zhou, P.; Fan, J.; Qiu, S. Study on Parameters of Two Widely Used Cohesive Soils Erosion Models. *Water* **2021**, *13*, 3621. https://doi.org/10.3390/w13243621

Received: 8 November 2021
Accepted: 12 December 2021
Published: 16 December 2021

Publisher's Note: MDPI stays neutral with regard to jurisdictional claims in published maps and institutional affiliations.

Copyright: © 2021 by the authors. Licensee MDPI, Basel, Switzerland. This article is an open access article distributed under the terms and conditions of the Creative Commons Attribution (CC BY) license (https://creativecommons.org/licenses/by/4.0/).

1. Introduction

Erosion models represent the constitutive law of soils for erosion problems, much like a stress–strain curve represents the constitutive law of soils for settlement problems. The most commonly used erosion models up to date are the excess shear stress model and the Wilson model. The excess stress shear model can be expressed as [1]:

$$\dot{z} = k_D(\tau - \tau_c)^{\alpha} \quad (1)$$

where $\dot{z}$ is the erosion rate (m s^{-1}), k_D is the coefficient of erodibility ($m^3/(N \times S)$), τ is the applied shear stress (Pa), τ_c is the critical shear stress (Pa), and α is an empirical exponent sometimes assumed to be unity [2–4]. Some scholars proposed dimensionless nonlinear excess shear stress models to calculate the erosion rate [1,5–7]. The typical dimensionless excess shear stress model is defined as:

$$\dot{z} = Z_0\left(\frac{\tau}{\tau_c} - 1\right)^{\alpha} \quad (2)$$

where Z_0 is the erodibility parameter of the dimensionless excess shear stress model (mm/h). However, it is difficult to predict the values of erodibility parameters due to the erodibility parameters (Z_0 and τ_c) changing with the season [8,9].

Wilson (1993a, 1993b) proposed a mechanistic detachment model to provide a general framework for studying soil and fluid characteristics [10,11]. The advantage of the

Wilson model over the over-shear stress model is that the factors affecting erosion can be considered and evaluated in greater depth; this has been studied extensively by related scholars, incorporating factors such as turbulence, roughness, seepage forces, material soil orientation, root effects, and negative pore water pressure effects into the Wilson model [12–16]. The Wilson model was based on the balance of all the forces and moments driving and resisting detachment that would be preferred for modeling the range of possible environmental conditions, which is expressed as:

$$\dot{z} = \frac{b_0\sqrt{\tau}}{\rho_b}\left[1 - \exp\left\{-\exp\left(3 - \frac{b_1}{\tau}\right)\right\}\right] \tag{3a}$$

$$b_0 = \rho_s \frac{k_r}{K_e}\sqrt{\frac{K_n}{k_{dd}(\rho_s - \rho_w)}} \tag{3b}$$

$$b_1 = \left(\frac{\pi}{e_v\sqrt{6}}\right)\frac{k_r(K_{ls} + f_c)}{K_d} g(\rho_s - \rho_w)d \tag{3c}$$

where ρ_b is the bulk density of soil (g m^{-3}), ρ_s and ρ_w are the densities of particle and water (1000 kg m^{-3}), respectively, K_e is the exposure of lower particle parameter, K_n is a combination and fluid factors, k_r is the ratio of k_v and k_a ($k_r = k_v/k_a = 2/3$), k_{dd} is detachment distance parameter, K_d is dimensionless hydraulic drag parameter, K_{ls} is the dimensionless bed and slope parameter that depends on particle (or aggregate) size, f_c is the dimensionless cohesive force parameter, and e_v is the coefficient of variation. Wilson suggested that the critical stress can be calculated by drag forces equaling time-average drag forces. The critical stress is expressed as:

$$\tau_c = \frac{k_r}{K_d}(\rho_s - \rho_w)dg(K_{ls} + f_c) \tag{4}$$

Al-Madhhachi (2013) tested the appropriateness of the excess stress shear model and Wilson model for cohesive sediment using flume tests, "mini" JET tests, and JET tests [12]. It was found that the Wilson model fitted the observed data from the original and "mini" JET better than the excess shear stress model, while it was consistent with the excess shear stress model in fitting the observations from the flume tests. Then, the seepage force was introduced into the Wilson model to improve the prediction effect of cohesive soil [17,18]. The recent Erosion Function Apparatus (EFA) test by Gao X et al. (2019) showed that the Wilson and shear stress models could also be applied to the test [19].

In the application of the scouring model, the determination of its parameters is a significant problem. Hanson and Cook (1997) and Hanson et al. (2002) developed analytical procedures to directly estimate k_D and τ_c based on diffusion principles of the circular jet scour test using an Excel spreadsheet [20,21]. Daly et al. (2013) proposed a new spreadsheet tool to solve for k_D and τ_c values simultaneously [22]. Al-Madhhachi et al. (2017) used the solver routine in Microsoft Excel to derive erodibility parameters b_0 and b_1, which utilized the generalized reduced gradient method [23]. Hanson and Simon (2001) found inversely proportional between the critical shear stress and the erodibility parameter k_D based on 83 jet-tests on cohesive streambeds in the Midwestern U.S., implying that one parameter can fully describe the soil erosion resistance [24]. An alternative relationship was proposed by Simon et al. (2011) based on hundreds of JETs on stream banks across the U.S [25]. However, other scholars found no correlation between erodibility parameter k_D and critical flow shear stress [26,27]. These studies have different views on the relationship between each parameter, which needs further confirmation. In addition, for the data set of the Erosion Function Apparatus test, whether the above relationship is applicable still needs further verification.

Erosion resistance of soil is closely related to its parameters such as soil gradation, compaction, clay content, etc. [28,29]; Briaud (2005) found that soil porosity ratio, water temperature, soil temperature, sodium adsorption ratio, and other parameters are directly

proportional to soil's erosion resistance ability [30], while soil specific gravity, plastic index, particle proportion with particle size <0.075 mm and other parameters are inversely proportional to soil's erosion resistance ability. The study shows that soil's physical and mechanical parameters closely affect its scour characteristics [29]. Therefore, soil properties play an essential role in soil erosion resistance. For the parameters in the scour model, it is also vital to determine their relationship with soil parameters. Hasan and Al-Madhhachi (2018) investigated the effect of crude oil on erosion parameters (b_0 and b_1) [13]. For clean soil and polluted soil, parameter b_1 increases with increasing water content. However, compared with clean soil, polluted soil has a more significant effect on parameter b_0. Al-Madhhachi (2013) proposed that the scouring parameter Z_0 is inversely proportional to water content in the scouring experiment of fine-grained soil [12]. In the scour experiment of silty clay and sand mixture, Z_0 and α are positively proportional to dry density and inversely proportional to the void ratio [19,31]. Although there has been some advance in studying erosion in cohesive soils, further research is needed to estimate erodibility parameters accurately.

In this study, a database of 177 cohesive soil erosion function apparatus tests with soil properties was collected from the literature review. The Wilson model and the dimensionless over-shear stress model were further extended for applications in EFA devices. The range of scouring parameters in the EFA data set is determined based on the experimental data and the theoretical derivation of erosion parameters. The values of the erosion parameters under EFA equipment are summarized. The general trend of erosion parameters and the relationship between erosion parameters are further illustrated. The variability of the parameters and the importance of each parameter are revealed. The relationship between soil erodibility parameters (b_0, Z_0, and α) and soil engineering properties is proposed by regression analysis, which could be helpful for computer simulation analysis of Scouring failure.

2. Methods

In the analysis of this paper, mean grain size and bulky soil density are normalized, and the data are converted into dimensionless data between 0 and 1. The remaining three parameters are expressed in decimal form, and then, regression analysis is conducted. The normalization formula is as follows:

$$x^* = \frac{x - x_{\min}}{x_{\max} - x_{\min}} \tag{5}$$

where x^* is the normalized data, and $x_{\max}$ and $x_{\min}$, respectively, represent the maximum and minimum values in this data group.

For the regression analysis model, the determination coefficient R^2 and F_{value} were used to evaluate the model's performance and determine the optimal parameter values [32,33]. The determination coefficient R^2 and F_{value} are defined as:

$$R^2 = 1 - \frac{\sum(y_i - \hat{y}_i)^2}{\sum(y_i - \overline{y})^2} \tag{6}$$

where y_i is the actual value of the sample, $\hat{y}_i$ is the fitting value, and $\overline{y}$ is the average value. *R-square* ranges from 0 to 1.0, which closer to 1.0 means better fit.

$$F_{value} = \frac{\sum(f_i - \overline{y})^2}{\sum(y_i - f_i)^2} \times (\frac{D}{V} - 1) \tag{7}$$

where D is the number of data points, and V is the number of independent variables. When the F_{value} is much higher than the critical value of the F test, the result of the regression equation is more reliable. The critical of F_{value} can be obtained from the F distribution table, and its significance level is set at 0.05.

Therefore, the combinations with higher R^2 and $F_{value}/F_{statistic}$ are chosen as equations relating the erodibility parameters to the soil geotechnical properties.

3. Erosion Function Apparatus Tests Database

The erosion function apparatus is currently one of the most commonly used soil erosion test equipment. It is used to investigate the erodibility of the non-cohesive soil, cohesive soil, and gravel. The EFA can measure the erosion rate curve and critical shear stress of cohesive soil [34].

The study collected a database of 177 tests. The coupling of various soil parameters influences the scour behavior of soil, and the scour mechanism is studied by investigating the influence of soil parameters on scouring behavior. The experimental data selected in this paper include the experimental data of scouring and soil parameters; some data lacking soil parameters are excluded. Among the database, eight tests were from Gao (2019), twelve tests were from ILIT (2006), eighty tests were from Shafii (2018), thirty-eight tests were from Briaud (1999, 2008), twelve tests were from Kwak (2000), six tests were from Park (2007), three tests were from Bernhardt (2011), five tests were from Govin (2009), and the thirteen tests were from Straub (2013) [19,28,35–42]. Table 1 shows the soil types according to the USCS classifications and the number of tests.

Table 1. List of the USCS classifications related to 177 texts.

USCS Classification	Number of Samples
Low-plasticity clay (CL)	99
High-plasticity clay (CH)	56
CH with sand	2
CL with sand	20

Figure 1 shows the soil samples main properties in the database, including plasticity index, percent fines, soil bulky density, water content, and mean grain size.

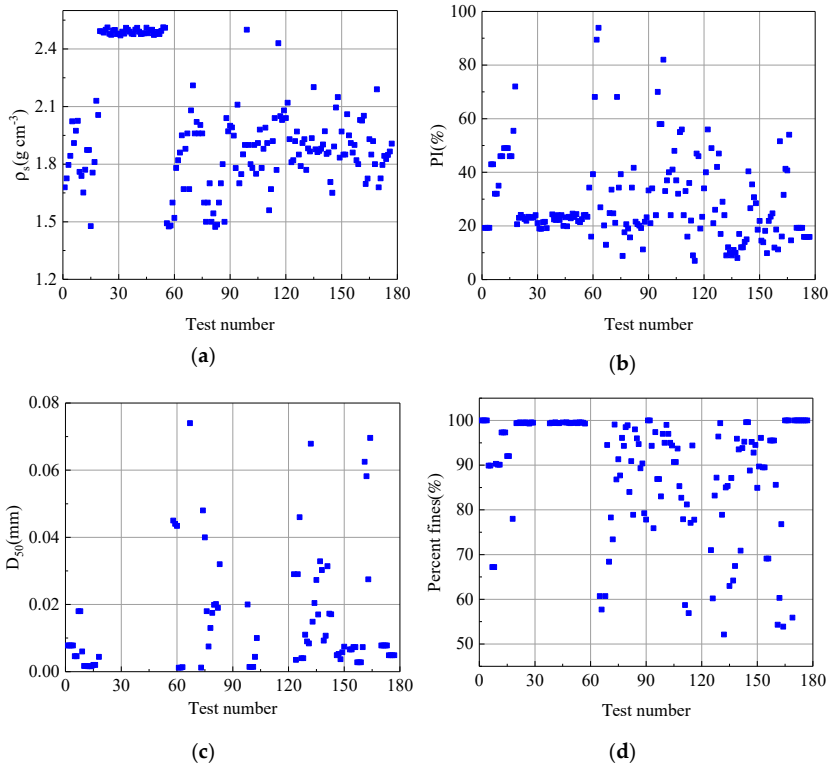
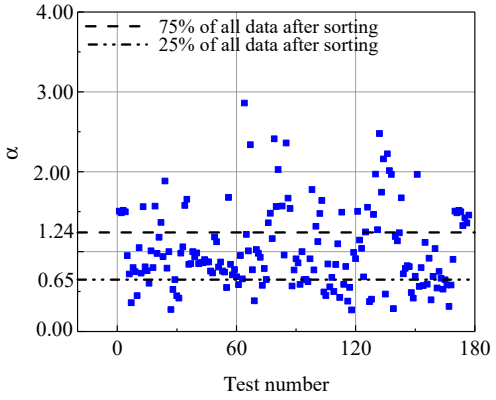


Figure 1. *Cont.*



(**c**)

Figure 1. Soil properties of samples: wet density (**a**); plasticity index (**b**); D_{50} (**c**); percent fines (**d**); water content (**e**).

4. Results and Discussion

4.1. The Data Range of the Experimental Erodibility Parameters Values

In this study, the Wilson model's erodibility parameters (b_0 and b_1) were derived using a curve fitting tool based on the principle of minimizing the error between predicted erosion data and measured erosion data. The critical shear stress τ_c is defined for this study as the interface shear stress corresponding to a very low erosion rate of 0.1 mm h^{-1}. The value of the erodibility parameter (Z_0) in equation 2 is equal to th e erosion rate when the hydraulic shear stress (τ) is equal to twice the critical shear stress (τ_c). After the critical shear stress and the erodibility parameter (Z_0) were determined, the exponential term (α) was estimated using the curve fitting tool by minimizing the sum of squared errors between the predicted erosion data and the measured erosion data. The erodibility parameters (τ_c, Z_0, and α) of the dimensionless excess shear stress model and the erodibility parameters (b_0 and b_1) of the Wilson model are shown in Figures 2 and 3, respectively.

The database was analyzed to obtain 177 Z_0, τ_c, α, b_0, and b_1 values. Figure 2 shows that the erodibility parameters Z_0, τ_c, and α of cohesive soils ranged from 0.10 mm h^{-1} to 117.23 mm h^{-1}, from 0.11 Pa to 50.25 Pa, and from 0.26 to 2.75, respectively. Briaud (2017) analyzed 84 EFA tests carried out by Texas A&M University and TxDOT and obtained the range of critical shear stress values for various soil types [43]. The range of critical shear stress of cohesive soils is 0.15–20 Pa obtained from Briaud (2017), which is consistent with the range of critical shear stress obtained in this paper. Several studies have shown that α varies between 1.0 and 6.8 [43–45], consistent with the range of α values obtained in the current paper.

Figure 3 shows that the erodibility parameters b_0 and b_1 values of cohesive soils ranged from 0.09 g m^{-1} s^{-1} $N^{-0.5}$ to 80.29 g $m^{-1}s^{-1}N^{-0.5}$ and from 0.56 Pa to 267.26 Pa, respectively. Based on equation 3b, it can be shown that the erodibility parameter b_0 is related to the bulk density of soil (ρ_b), the densities of the particle (ρ_s), the ratio of volume/area parameters (k_r), the exposure of lower particle parameter (K_e), a combination and fluid factors (K_n), and detachment distance parameter (k_{dd}). Wilson recommended that Wilson recommended that $kr = 2/3$ for spherical particles, $k_{dd} = 2$. Wilson (1993b) defines a combination and fluid factors (K_n) as [11]:

$$K_n = K_t K_d / k_r \tag{8}$$

where K_t is the cumulation of instantaneous force. Wilson suggested that $K_t = 2.5$ and the dimensionless hydraulic drag parameter (K_d) is defined as:

$$K_{\mathrm{d}} = \frac{C_d k_f [\ln(\varphi)/\kappa + B]^2}{2} \tag{9}$$

where C_d is the drag coefficient, Einstein and El-Samni (1949) suggested that the value of C_d is 0.2 [46]; k_f is the fraction of exposed area, and Wilson recommended a value of 0.92; φ is the drag velocity fractional height, Einstein and El-Samni (1949) suggested $\varphi = 0.35$, while Yang (1973) suggested $\varphi = 1$ [46,47]; κ is the von Kannon constant, Wilson recommended $\kappa = 0.4$; B is the Log-velocity intercept parameter which ranges from 6.5 to 9.8 [11]. The maximum value of K_d is 8.84, and the minimum value is 1.38. Therefore, the maximum value of K_n is 33.15. Kothyari (2008) suggested that the density value of clay is 2.7 g cm^{-3} [48]. The influence of the exposure factor k_e on the erosion parameter b_0 is critical, but little information is available directly on the parameter k_e [11,12]. The method of determination of this parameter needs to be further studied.

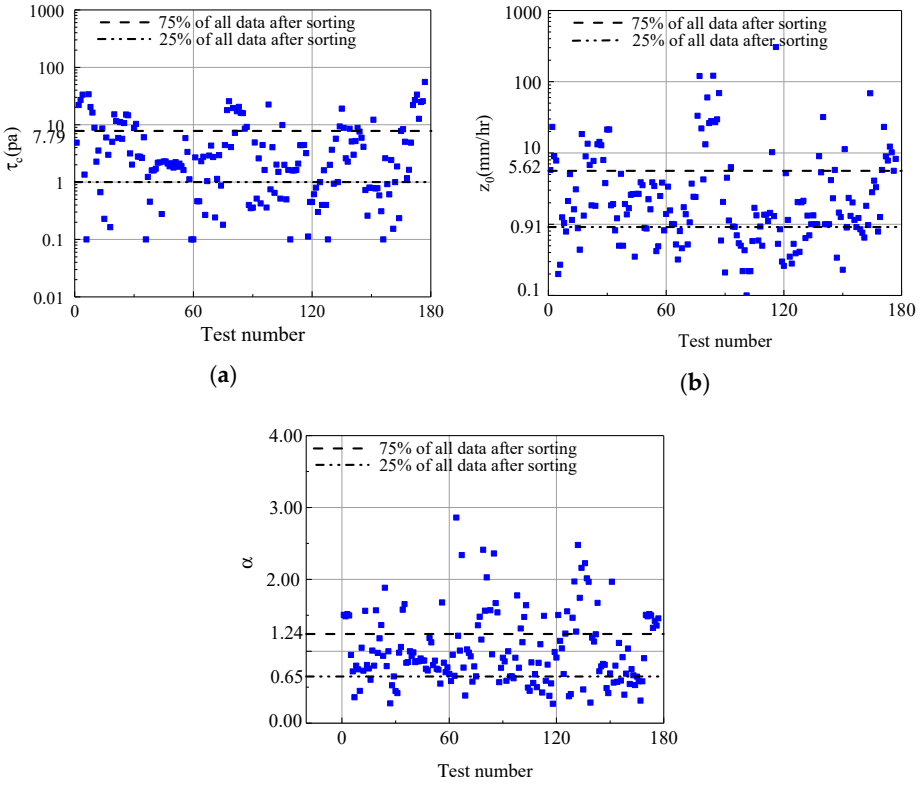


Figure 2. Erodibility parameters of the excess stress shear model: the critical shear stress (τ_c) (**a**); the erodibility parameters Z_0 (**b**); an empirical exponent α (**c**).

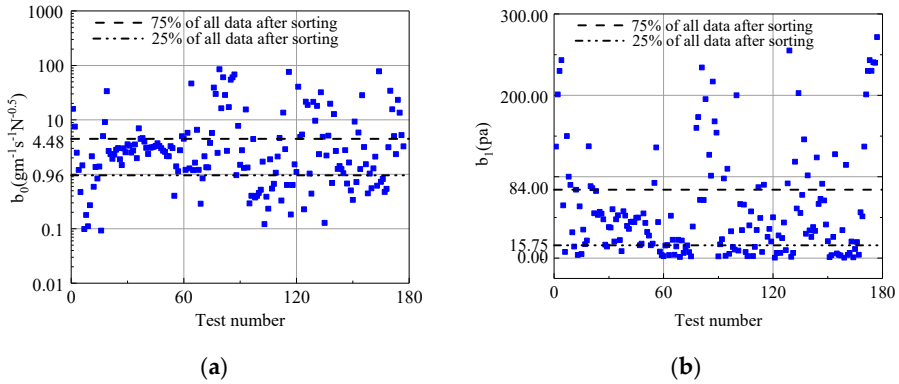


Figure 3. Erodibility parameters of the Wilson model: the erodibility parameters b_0 (**a**); the erodibility parameters b_1 (**b**).

To obtain the maximum value of parameter b_1, combine Equations (3c) and (4):

$$b_{1(\max)} = \frac{\pi \tau_{c(\max)}}{e_v \sqrt{6}} \tag{10}$$

The value of e_v in this study is 0.35. Due to the maximum value of τ_c being 50.25 Pa obtained from the database, the theoretical maximum value of b_1 is 184.04 Pa. We can find that the range of theoretical values of the erodibility parameters (b_0 and b_1) includes the experimental values.

A comparison of erodibility parameters between high-plasticity clay (CH: $PI \geq 0.73(w_L\text{-}20)$, $PI \geq 7$, and $w_L \geq 50$) and low-plasticity clay (CL:PI ≥ 0.73 (w_L-20), $PI \geq 7$, and $w_L < 50$) is shown in Figures 4 and 5. Compared with the erodibility parameter b_0 of high-plasticity clay, the erodibility parameter b_0 of low-plasticity clay is higher. The range of erodibility parameters b_0 of high-plasticity clay and low-plasticity clay mainly concentrates in 0.44–2.77 g m^{-1} s^{-1} N$^{-0.5}$ and 1.35–4.6 g m^{-1} s^{-1} N$^{-0.5}$, respectively (Figure 4a). The erodibility parameter b_0 decrease with the water content increase due to the rise of soil cohesion (which increases K_e). Similar observations are reported for Z_0. The range of erodibility parameters Z_0 of high-plasticity clay and low-plasticity clay is mainly concentrated in 0.5–3.31 mm h^{-1} and 1–8.94 mm h^{-1}, respectively (Figure 5b). The range of erodibility parameters Z_0 of low-plasticity is higher than the range of erodibility parameters Z_0 of high-plasticity. Therefore, b_0 has a similar relationship with z_0 relative to the liquid limit (Figures 4a and 5b).

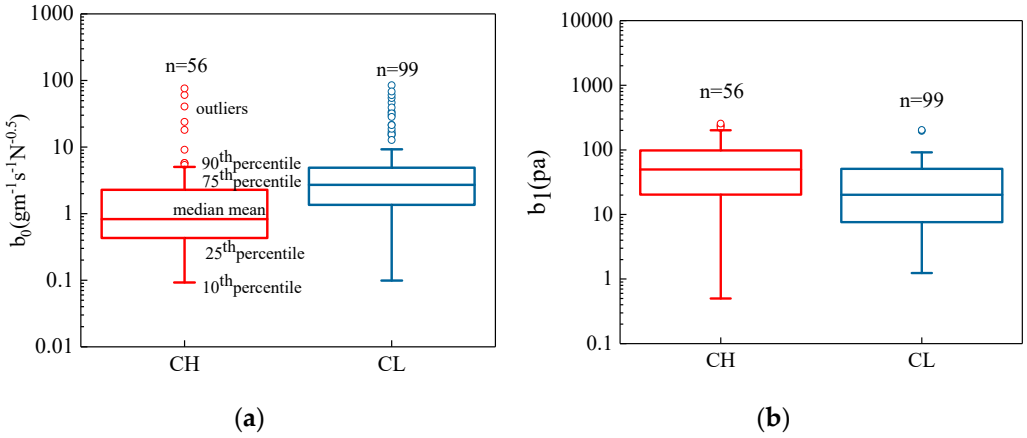


Figure 4. The range of derived parameters b_0 (**a**) and b_1 (**b**) for high-plasticity clay and low-plasticity clay.

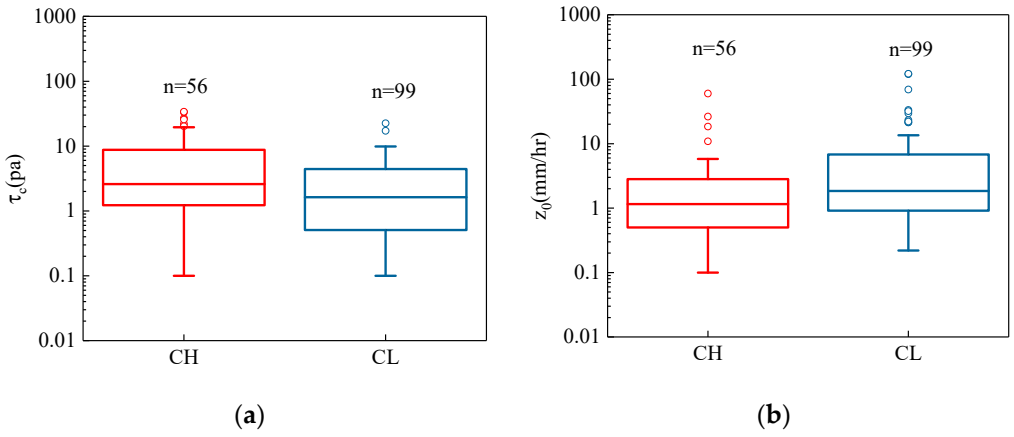


Figure 5. The range of derived parameters τ_c (**a**) and Z_0 (**b**) for high-plasticity clay and low-plasticity clay.

Compared with the erodibility parameter b_1 of high-plasticity clay, the erodibility parameter b_1 of low-plasticity clay is lower. The erodibility parameter b_1 decreased as the liquid limit increased due to increasing soil cohesion (which increases *fc*). The range of erodibility parameters b_1 of high-plasticity is mainly concentrated in 20.33–97.82 Pa, whereas the range of parameters b_1 of low-plasticity clay is concentrated in 0.44–50.2 Pa (Figure 4b). Similar observations are reported for $\tau_{c.}$ The τ_c increase as the liquid limit increase due to increasing cohesion. The range of the τ_c of high-plasticity clay experimental data is mainly concentrated in 1.23–8.78 Pa, whereas the range of the critical shear stress of low-plasticity clay is primarily concentrated in 0.5–4.43 Pa (Figure 5a). We can find that the range of erodibility parameters τ_c of low-plasticity is lower than the range of erodibility parameters τ_c of high-plasticity. Therefore, b_1 has a similar relationship with τ_c relative to the liquid limit (Figures 4a and 5b).

4.2. Relation between z_0 and τ_c and between b_0 and b_1

As it is meaningful to explore whether there is a relationship between Z_0 and τ_c and between b_0 and b_1, all datasets from each author have been plotted individually (Figures 6 and 7). When the research data samples are small for the over-shear stress model, the discreteness between parameter Z_0 and over-shear stress τ_c is significant (Figure 6a,b). In the case of sufficient data, the results of Shafii (2018) and Briaud (1999, 2008) showed that there was a direct proportional linear relationship between the parameter Z_0 and τ_c. Additionally, this result has been confirmed in the research results of Hanson and Simon (2001), as shown in Figure 6c,d.

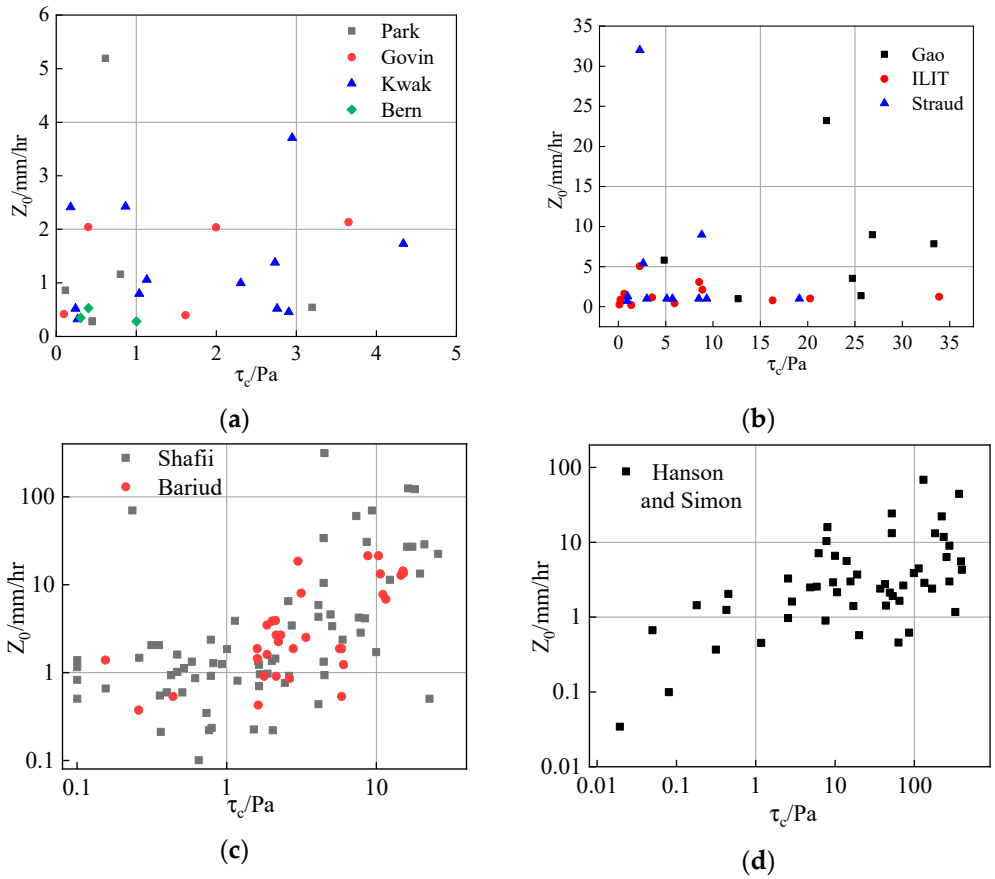


Figure 6. The erodibility coefficient (Z_0) as a function of critical flow shear stress (τ_c) under identical experimental conditions: Sub-dataset 1 (**a**), Sub-dataset 2 (**b**), Sub-dataset 3 (**c**), and Sub-dataset 4 (**d**).

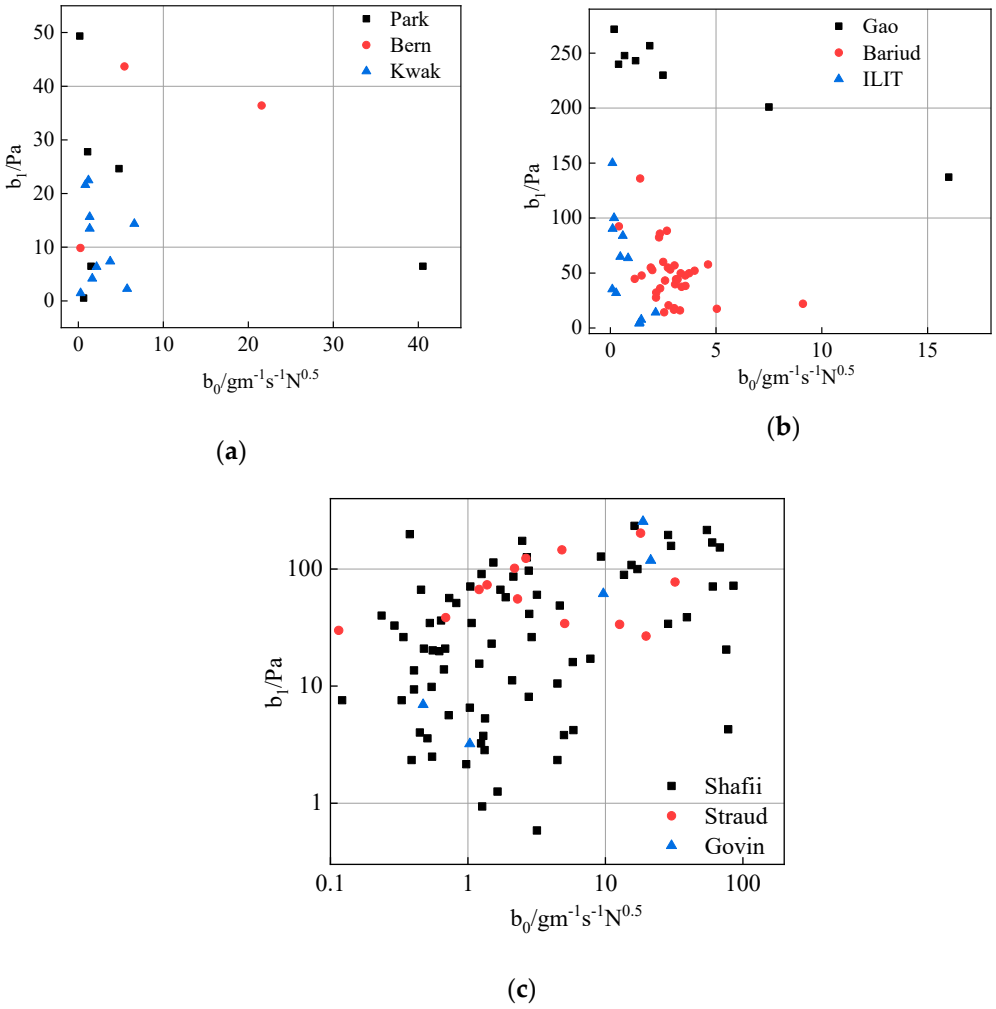


Figure 7. The erodibility parameter b_1 as a function of the erodibility b_0 under identical experimental conditions: Sub-dataset 1 (**a**), Sub-dataset 2 (**b**), and Sub-dataset 3 (**c**).

When the Wilson model is studied, this trend does not exist between b_0 and b_1. As shown in Figure 7a, b_1 and b_0 are highly discrete. While the number of data increases, the study samples of Gao (2019), Briaud (1999, 2008), and ILIT (2006) show an inverse proportional linear between the two parameters (Figure 7b). Criswell et al. (2016) also found an inverse relationship between b_0 and b_1 for gravels. However, this relationship is not confirmed in the studies of Shafii (2018), Straud (2013), and Govin (2009) (Figure 7c), which proves that there is no such relationship between parameters b_0 and b_1.

4.3. Multiple Nonlinear Regression Analysis

The multiple nonlinear model is used to study equations relating the erodibility parameters b_0 and Z_0 to the soil geotechnical properties in this research. The multiple no-nlinear model is shown in Equation (11):

$$Y = A \times (P_1)^{\alpha_1} \times (P_2)^{\alpha_2} \times (P_3)^{\alpha_3} \times \cdots \times (P_n)^{\alpha_n} \quad (11)$$

where Y is the dependent variable; P_n is the soil geotechnical properties, including plasticity index, percent fines, wet density, water content, and mean grain size in this case. Many combinations between the erodibility parameters and the soil geotechnical properties can be selected to generate regression equations.

The correlation analysis of soil parameters and scour parameters in the database is carried out. The analysis results are shown in the following table. The correlation coefficient

between soil parameter *PI*, *WC*, D_{50}, and scour parameters is significant, so these three parameters can be used to analyze the relationship with scouring parameters.

According to the results of correlation analysis, we conducted regression analysis on *WC*, *PI*, and D_{50}, with R^2 and F test indexes as evaluation indexes. Table 2 summarizes the best regression equations for the erodibility parameters (b_0, α, and Z_0) of cohesive soils. According to Table 3, the relationship between parameters b_0, α, and Z_0 with the selected soil parameters is similar. They are inversely proportional to the plasticity index but directly proportional to water content and median grain size, which is consistent with the results of correlation analysis in Table 2. Figure 8a–c shows the comparison of predicted and measured values of the three parameters.

Table 2. Correlation analysis results of scouring parameters and soil parameters.

Parameter	b_0	b_1	Z_0	τ_c	α
PI	−0.392 **	0.004	−0.231	0.056	−0.371 **
ρ_s	−0.172	−0.107	−0.316 **	−0.069	−0.085
WC	0.141	0.393 **	0.304 **	0.333 **	0.593 **
P_f	−0.032	0.130	−0.081	0.043	0.077
D_{50}	0.439 **	−0.114	0.391 **	−0.116	0.076

Note: The number in the table represents the correlation between parameters, ** represents significant correlation, and the significance level is 0.01.

Table 3. Results of multiple nonlinear regression.

Dependent Variable	Model Expression	Number of Data	R^2	$F_{value}/F_{statistic}$
b_0 (g m^{-1} s^{-1} N$^{-0.5}$)	$b_0 = 3.66 \times WC^{1.65} \times PI^{-0.53} \times D_{50}{}^{0.72}$	54	0.63	10.82
Z_0 (mm h^{-1})	$z_0 = 0.123 \times WC^{2.37} \times PI^{-0.86} \times D_{50}{}^{0.39}$	54	0.63	9.23
α	$\alpha = 0.094 \times WC^{1.26} \times PI^{-0.19} \times D_{50}{}^{0.25}$	54	0.67	92.21

Note: D_{50} (mm)—mean particle size; *WC* (%)—water content; *PI* (%)—plastic index.

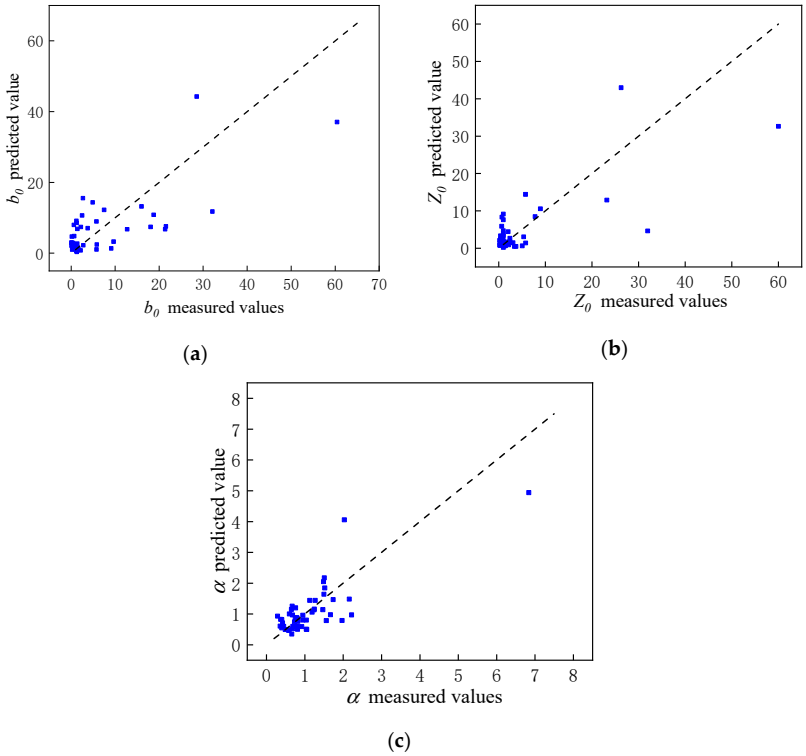


Figure 8. The results of b_0 (**a**); b_1 (**b**) and α (**c**) regression analysis were compared with the measured values.

5. Conclusions

A database of 177 EFA tests of cohesive soils with soil properties is present. The database is used to derive the erodibility parameters (Z_0, τ_c, and α) of the dimensionless excess shear stress model and the erodibility parameters (b_0 and b_1) of the Wilson model to obtain a new database of 177 erodibility parameters (Z_0, τ_c, α, b_0, and b_1). The new database is used to determine the range of all erodibility parameters (Z_0, τ_c, α, b_0, and b_1). The parameters Z_0, τ_c, and α values of cohesive soils ranged from 0.10 mm h^{-1} to 117.23 mm h^{-1}, from 0.11 Pa to 50.25 Pa, and from 0.26 to 2.75, respectively. The parameters b_0 and b_1 of cohesive soils ranged from 0.09 g m^{-1} s^{-1} $N^{-0.5}$ to 50.25 g m^{-1} s^{-1} $N^{-0.5}$ and from 0.56 Pa to 267.26 Pa, respectively.

The new databases were categorized according to the USCS (Briaud, 2013) classifications [49]. It found that the range of Z_0, τ_c, b_0 and b_1 values of high-plasticity clay is mainly concentrated in 0.5–3.31 mm h^{-1}, 1.23–8.78 Pa, 0.44–2.77 g m^{-1} s^{-1} $N^{-0.5}$, and 20.33–97.82 Pa, respectively, whereas the range of Z_0, τ_c, b_0, and b_1 values of low-plasticity clay are mainly concentrated in 1–8.94 mm h^{-1}, 0.5–4.43 Pa, 1.35–4.6 g m^{-1} s^{-1} $N^{-0.5}$, and 0.44–50.2 Pa. The experimental values obtained from the low-plasticity clay show that the τ_c and b_1 values are lower than the high-plasticity clay values. In comparison, their Z_0 and τ_c values are higher than the high-plasticity clay values. Therefore, erodibility parameters b_0 and b_1 have a similar relationship with Z_0 and τ_c relative to the liquid limit, respectively.

The new databases are also used to develop regression equations that link the erodibility parameters (Z_0 and b_0) to the index soil parameters, such as the mean grain size, the water content, the percent fines, the plasticity index, the bulk density, and the plastic limit. It is found that z_0 and b_0 values consistently decreased when the plasticity index increased, while water content and mean grain size decreased. Therefore, the Wilson model parameter b_0 had a similar relationship but a different magnitude, as parameter Z_0 relative to the water content, the mean grain size, and the plasticity index. These results apply to EFA devices and may not be applicable to other devices such as jet erosion tests and hole erosion tests.

Author Contributions: All authors contributed extensively to the work presented in this paper. Conceptualization, Q.W.; Funding acquisition, Q.W.; Investigation, J.F.; Methodology, Q.W.; Project administration, Q.W.; Supervision, S.Q.; Validation, P.Z.; Visualization, P.Z.; Writing—original draft, J.F.; Writing—review and editing, P.Z. All authors have read and agreed to the published version of the manuscript.

Funding: This research was funded by National Natural Science Foundation of China, grant number 52130905; 51679003 and the APC was funded by 51679003.

Institutional Review Board Statement: Not applicable.

Informed Consent Statement: Informed consent was obtained from all subjects involved in the Study.

Data Availability Statement: The data were obtained from the summary of other scholars' research papers; all data can be obtained from the figures of this paper.

Acknowledgments: This work was financially supported by the National Natural Science Foundation of China (Grant No. 52130905; No.51679003). The authors want to thank the anonymous reviewers and editors for their valuable comments and suggestions that significantly contributed to this manuscript's improvement.

Conflicts of Interest: The authors declare no conflict of interest.

References

1. Partheniades, E. Erosion and deposition of cohesive soils. *J. Hydraul. Div. ASCE* **1965**, *91*, 105–139. [CrossRef]
2. Hanson, G.J. Surface erodibility of earthen channels at high stresses part I-open channel testing. *Trans. ASAE* **1990**, *33*, 127–131. [CrossRef]
3. Hanson, G.J. Surface erodibility of earthen channels at high stresses part II-developing an in situ testing device. *Trans. ASAE* **1990**, *33*, 132–137. [CrossRef]

4. Hanson, G.J.; Cook, K.R. Apparatus, test procedures, and analytical methods to measure soil erodibility in situ. *Appl. Eng. Agric.* **2004**, *20*, 455–462. [CrossRef]
5. Gailani, J.; Ziegler, C.K.; Lick, W. Transport of suspended solids in the Lower Fox River. *J. Great Lakes Res.* **1991**, *17*, 479–494. [CrossRef]
6. Lin, Q.; Wu, W. A one-dimensional model of mixed cohesive and non-cohesive sediment transport in open channels. *J. Hydraul. Res.* **2013**, *51*, 506–517. [CrossRef]
7. Wicks, J.M.; Bathurst, J.C. SHESED: A physically based, distributed erosion and sediment yield component for the SHE hydrological modelling system. *J. Hydrol.* **1996**, *175*, 213–238. [CrossRef]
8. Henderson, M.B.; Wynn, T.M.; Vaughn, D.H. Changes in streambank erodibility and critical shear stress due to subaerial processes. In Proceedings of the 2006 ASABE Annual Meeting American Society of Agricultural and Biological Engineers, Portland, OR, USA, 9–12 July 2006.
9. Wynn, T.M.; Henderson, M.B.; Vaughn, D.H. Changes in streambank erodibility and critical shear stress due to subaerial processes along a headwater stream, southwestern Virginia, USA. *Geomorphology* **2007**, *97*, 260–273. [CrossRef]
10. Wilson, B.N. Development of a fundamentally based detachment model. *Trans. ASAE* **1993**, *36*, 1105–1114. [CrossRef]
11. Wilson, B.N. Evaluation of a fundamentally based detachment model. *Trans. ASAE* **1993**, *36*, 1115–1122. [CrossRef]
12. Al-Madhhachi, A.T.; Hanson, G.J.; Fox, G.A.; Tyagi, A.K.; Bulut, R. Deriving parameters of a fundamental detachment model for cohesive soils from flume and jet erosion tests. *Trans. ASABE* **2013**, *56*, 489–504. [CrossRef]
13. Hasan, M.B.; Al-Madhhachi, A.T. The influence of crude oil on mechanistic detachment rate parameters. *Geosciences* **2018**, *8*, 332. [CrossRef]
14. Abbood, A.A.; Al-Madhhachi, A.T. Quantifying mechanistic detachment parameters due to humic acids in biological soil crusts. *Land* **2021**, *10*, 1180. [CrossRef]
15. Al-Madhhachi, A.T.; Mutter, G.M.; Hasan, M.B. Predicting mechanistic detachment model due to Lead-Contaminated soil treated with Iraqi Stabilizers. *KSCE J. Civ. Eng.* **2019**, *23*, 2898–2907. [CrossRef]
16. Criswell, D.T.; Al-Madhhachi, A.T.; Fox, G.A.; Miller, R.B. Deriving erodibility parameters of a mechanistic detachment model for gravels. *Trans. ASABE* **2016**, *59*, 145–151.
17. Al-Madhhachi, A.T.; Fox, G.A.; Hanson, G.J. Quantifying the erodibility of streambanks and hillslopes due to surface and subsurface forces. *Trans. ASABE* **2014**, *57*, 1057–1069.
18. Al-Madhhachi, A.T.; Fox, G.A.; Hanson, G.J.; Tyagi, A.K.; Bulut, R. Mechanistic detachment rate model to predict soil erodibility due to fluvial and seepage forces. *J. Hydraul. Eng.* **2014**, *5*, 04014010. [CrossRef]
19. Gao, X.; Wang, Q.; Ma, G. Experimental investigation on the erosion threshold and rate of gravel and silt clay mixtures. *Trans. ASABE* **2019**, *62*, 867–875. [CrossRef]
20. Hanson, G.J.; Cook, K.R. Development of excess shear stress parameters for circular jet testing. In Proceedings of the American Society of Agricultural Engineers Meetings Papers, Minneapolis, MN, USA, 10–14 August 1997.
21. Hanson, G.J.; Robinson, K.M.; Cook, K.R. Scour below an overfall: Part II. Prediction. *Trans. ASAE* **2002**, *45*, 957–964. [CrossRef]
22. Daly, E.R.; Fox, G.A.; Al-Madhhachi, A.T.; Miller, R.B. A scour depth approach for deriving erodibility parameters from jet erosion tests. *Trans. ASABE* **2013**, *56*, 1343–1351.
23. Al-Madhhachi, A.T. Variability in soil erodibility parameters of Tigris Riverbanks using linear and non-linear models. *Al-Nahrain J. Eng. Sci.* **2017**, *20*, 959–969.
24. Hanson, G.J.; Simon, A. Erodibility of cohesive streambeds in the loess area of the Midwestern USA. *Hydrol. Process.* **2001**, *15*, 23–38. [CrossRef]
25. Simon, A.; Bankhead, N.L.; Thomas, R.E. Development and application of a deterministic Bank-Stability and Toe-Erosion Model (BSTEM) for stream restoration. In *Stream Restoration in Dynamic Systems: Scientific Approaches, Analyses, and Tools*; American Geophysical Union: Washington, DC, USA, 2011; pp. 453–474.
26. Laflen, J.M.; Elliot, W.J.; Simanton, J.R.; Holzey, C.S.; Kohl, K.D. WEPP Soil erodibility experiments for rangeland and cropland soils. *J. Soil Water Conserv.* **1991**, *46*, 39–44.
27. Mamo, M.; Bubenzer, G.D. Detachment rate, soil erodibility and soil strength as influenced by living plant roots part II: Field study. *Trans. ASAE* **2001**, *44*, 1175–1181. [CrossRef]
28. Bernhardt, M.L. 2008 Midwest Levee Failure: Erosion Studies. Ph.D. Thesis, Texas A&M University, College Station, TX, USA, 2011.
29. Kimiaghalam, N.; Clark, S.P.; Ahmari, H. An experimental study on the effects of physical, mechanical, and electrochemical properties of natural cohesive soils on critical shear stress and erosion rate. *Int. J. Sediment Res.* **2016**, *31*, 1–15. [CrossRef]
30. Briaud, J.L. Erodibility of fine grained soils and new soil test. In *Erosion of Soils and Scour of Foundations*; Geo-Frontiers Congress: Austin, TX, USA, 2005; pp. 1–10.
31. Wang, Q.S.; Su, R.L.; Gao, X.J. Study on the starting test of remolded clay soils and soils with different sand and gravel contents. *J. Hydraul. Eng.* **2018**, *49*, 975–985.
32. Pennell, K.D.; Hornsby, A.G.; Jessup, R.E.; Rao, P.S.C. Evaluation of five simulation models for predicting aldicarb and bromide behavior under field conditions. *Water Resour. Res.* **1990**, *26*, 2679–2693. [CrossRef]
33. Hession, W.C.; Shanholtz, V.O.; Mostaghimi, S.; Dillaha, T.A. Uncalibrated performance of the finite element storm hydrograph model. *Trans. ASAE* **1994**, *37*, 777–783. [CrossRef]

34. Briaud, J.L.; Chen, H.C. Erosion function apparatus for scour rate prediction. *J. Geotech. Geoenviron. Eng.* **2001**, *127*, 105–113. [CrossRef]
35. Team, I.L.I. Investigation of the Performance of the New Orleans Flood Protection Systems in Hurricane Katrina on August 29, 2005. 2006. Available online: https://digitalcommons.calpoly.edu/cgi/viewcontent.cgi?article=1032&context=cenv_fac (accessed on 12 December 2021).
36. Shafii, I. Relationship between Erodibility and Properties of Soils. Ph.D. Thesis, Texas A&M University, College Station, TX, USA, 2018.
37. Briaud, J.L. Case histories in soil and rock erosion: Woodrow wilson bridge, Brazos River Meander, Normandy Cliffs, and New Orleans Levees. *J. Geotech. Geoenviron. Eng.* **2008**, *134*, 1425–1447. [CrossRef]
38. Briaud, J.-L.; Ting, F.C.K.; Chen, H.C.; Gudavalli, R.; Perugu, S.; Wei, G. SRICOS: Prediction of Scour Rate in Cohesive Soils at Bridge Piers. *J. Geotech. Geoenviron. Eng.* **1999**, *125*, 237–246. [CrossRef]
39. Kwak, K. Prediction of Scour Depth versus Time for Bridge Piers in Cohesive Soils in the Case of Multi-Flood and Layered Soil Systems. Ph.D. Thesis, Texas A&M University, College Station, TX, USA, 2000.
40. Park, N. A Prediction of Meander Migration Based on Large-Scale Flume Tests in Clay. Ph.D. Thesis, Texas A&M University, College Station, TX, USA, 2007.
41. Govin-dasamy, A.V. Simplified Method for Estimating Future Scour Depth at Existingbridges. Ph.D. Thesis, Texas A&M University, College Station, TX, USA, 2009.
42. Straub, T.D.; Over, T.M.; Domanski, M.M. *Ultimate Pier and Contraction Scour Prediction in Cohesive Soils at Selected Bridges in Illinois*; National Technical Information Service: Springfield, VA, USA, 2013.
43. Briaud, J.L.; Govindasamy, A.V.; Shafii, I. Erosion charts for selected geomaterials. *J. Geotech. Geoenviron. Eng.* **2017**, *143*, 04017072. [CrossRef]
44. Van Klaveren, R.W.; McCool, D.K. Erodbility and critical shear of a previously frozen soil. *Trans. ASAE* **1998**, *41*, 1315–1321. [CrossRef]
45. Knapen, A.K.; Poesen, J.; Govers, G.; Gyssels, G.; Nachtergaele, J. Resistance of soils to concentrated flow erosion: A review. *Earth-Sci. Rev.* **2007**, *80*, 75–109. [CrossRef]
46. Einstein, H.A.; El-Samni, E.A. Hydrodynamic forces acting on a rough wall. *Rev. Mod. Phys.* **1949**, *21*, 520–524. [CrossRef]
47. Yang, C.T. Incipient motion and sediment transport. *J. Hydraul. Div.* **1973**, *99*, 1679–1704. [CrossRef]
48. Kothyari, U.C.; Jain, R.K. Influence of cohesion on the incipient motion condition of sediment mixtures. *Water Resour.* **2008**, *44*, W04410. [CrossRef]
49. Briaud, J.L. *Geotechnical Engineering: Unsaturated and Saturated Soils*; John Wiley & Sons: Hoboken, NJ, USA, 2013.